groups (subfamilies). For more details, see also Evans & Guggenheim (1988).

The chlorite–vermiculite group: There are two kinds of octahedral sheets in these structures: the *Oc* sandwiched between two *Tet* and the *interlayer* (Fig. 9.2.2.14). The structures belong to category IV. Any *Oc* can be independently homo-, meso-, or hetero-octahedral, and thus, theoretically, there are nine families here. Although vermiculites have a crystal chemistry different from chlorites, they can be, from the symmetry point of view, treated together. There are 20 (24) homo-homo-octahedral, 44 (60) homo-meso-octahedral and 164 (256) meso-meso-octahedral MDO polytypes (the first prefix refers to the 2:1 layer, the second to the interlayer); the other families have not yet been treated. Some of these polytypes have also been derived by other authors (for references, see Bailey, 1980; Zvyagin *et al.*, 1979).

In order to preserve a unitary system, some monoclinic polytypes necessitate a 'third' setting, with the *a* axis unique. These should not be transformed into the standard second setting.

9.2.2.3.1.2. *Diffraction pattern and identification of individual polytypes*

Owing to the trigonal symmetry of the basic structural units and their stacking mode, the single-crystal diffraction pattern of hydrous phyllosilicates has a hexagonal *geometry* and it can be referred to hexagonal or orthohexagonal reciprocal vectors $\mathbf{a}_1^*$, $\mathbf{a}_2^*$ or $\mathbf{a}^*$, $\mathbf{b}^*$, respectively (Figs. 9.2.2.15 and 9.2.2.16). It contains three types of diffractions:

(1) Diffractions 00*l* (or 000*l*), always sharp and common to all polytypes of a family including all its subfamilies. They are indicative of the mineral group, but useless for the identification of polytypes.

(2) The remaining diffractions with $k_{\rm ort} \equiv 0 \pmod 3$, always sharp and common to all polytypes of the same subfamily.

(3) All other diffractions: sharp only for periodic polytypes, otherwise present on diffuse rods parallel to $\mathbf{c}^*$. These are characteristic of individual polytypes. Diffractions 0*kl* – if sharp – are common to all polytypes of the family with the same *bc* projection.

From descriptive geometry, it is known that two orthogonal projections suffice to characterize unambiguously any structure and, therefore, the superposition structure (which implicitly contains the *ac* projection) together with the *bc* projection suffice for an unambiguous characterization of any polytype. It also follows that the diffractions with $k \equiv 0 \pmod 3$ together with the 0*kl* diffractions with $k \not\equiv 0 \pmod 3$ suffice for its determination (except for homometric structures) (Ďurovič, 1981).

From the trigonal or hexagonal symmetry of any superposition structure and from Friedel's law, it follows that the reciprocal rows 20*l*, 13*l*, $\bar{1}3l$, $\bar{2}0l$, $\bar{1}\bar{3}l$, and $1\bar{3}l$ (Fig. 9.2.2.16) carry the same information. Therefore, for identification purposes, it suffices to calculate the distribution of intensities along the reciprocal rows 20*l* (superposition structure – subfamily) and 02*l* (*bc* projection) for all MDO polytypes. Experience shows (Weiss & Ďurovič, 1980) that a mere visual comparison of calculated and observed intensities along these two rows suffices for an unambiguous identification of a MDO polytype. A similar scheme has been presented by Bailey (1988*b*).

The above considerations are based on the ideal Radoslovich model. Diffraction patterns of real structures may exhibit deviations owing to the distortion of the ideal lattice geometry and/or symmetry of the structure.

9.2.2.3.2. *Stibivanite Sb_2VO_5*

The crystal structure of this mineral has been determined by Szymański (1980). It turned out to be identical with that of the compound of the same composition synthesized earlier (Darriet, Bovin & Galy, 1976). The structure is monoclinic with space group $C12/c1$, lattice parameters $a = 17.989\ (6)$, $b = 4.7924\ (7)$, $c = 5.500\ (2)$ Å, $\beta = 95.13\ (3)^\circ$.

Structural units are formed of SbO_2–O–VO–O–SbO_2 extended along **a**, with adjacent units bonded along **c** through Sb—O—Sb and V—O—V bonds. Ribbons are thus formed with no bonding along **b**, and only the Sb—O interactions [2.561 (4) Å] along **a** (Fig. 9.2.2.17). This accounts for the excellent acicular cleavage.

Merlino *et al.* (1989) recognized in this structure sheets of VO_5 square pyramids (*Pyr*) parallel to **bc**, with layer symmetry $P(2/m)2/c2_1/m$ alternating with sheets containing chains of distorted SbO_3 tetrahedron-like pyramids (*Tet*) with layer symmetry $P(1)2_1/c1$ (Fig. 9.2.2.18). Owing to the higher symmetry of *Pyr*, they concluded that there may also exist an alternative attachment of *Tet* to *Pyr*, such that the triples (*Tet*; *Pyr*; *Tet*) will exhibit the layer symmetry $Pmc2_1$, and they will be arranged so that another polytype 2*O* with symmetry $P2_1/m2_1/c2_1/n$ (Fig. 9.2.2.19) is formed [in the original 2*M* polytype, the triples (*Tet*; *Pyr*; *Tet*) have the layer symmetry $P(1)2/c1$]. A mineral with such a structure, with lattice parameters $a = 17.916\ (3)$, $b = 4.700\ (1)$, $c = 5.509\ (1)$ Å, has actually been found.

The polytypism of stibivanite is reflected in its OD character: the two kinds of sheets *Pyr* and *Tet* correspond to two kinds of non-polar layers: their relative position is given by the family symbol:

$$\begin{matrix} P(1)2_1/c1 & P(m)cm \\ [1/4, -0.0733\ldots] & \text{category IV,} \end{matrix}$$

the *NFZ* relations being

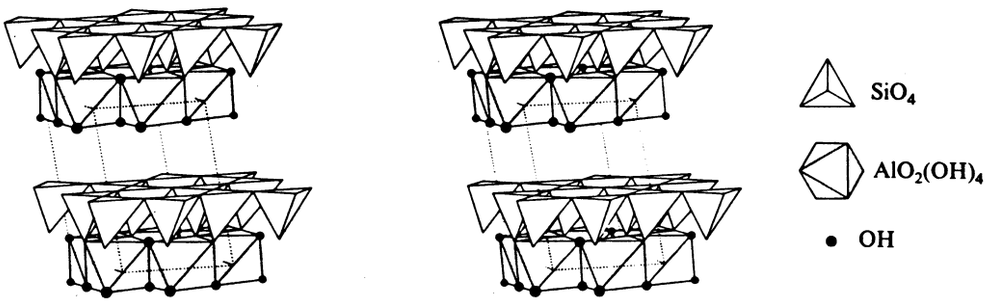

Fig. 9.2.2.11. Stereopair showing the sequence of sheets in the structures of the serpentine–kaolin group (kaolinite-1*A*, courtesy Zoltai & Stout, 1985).

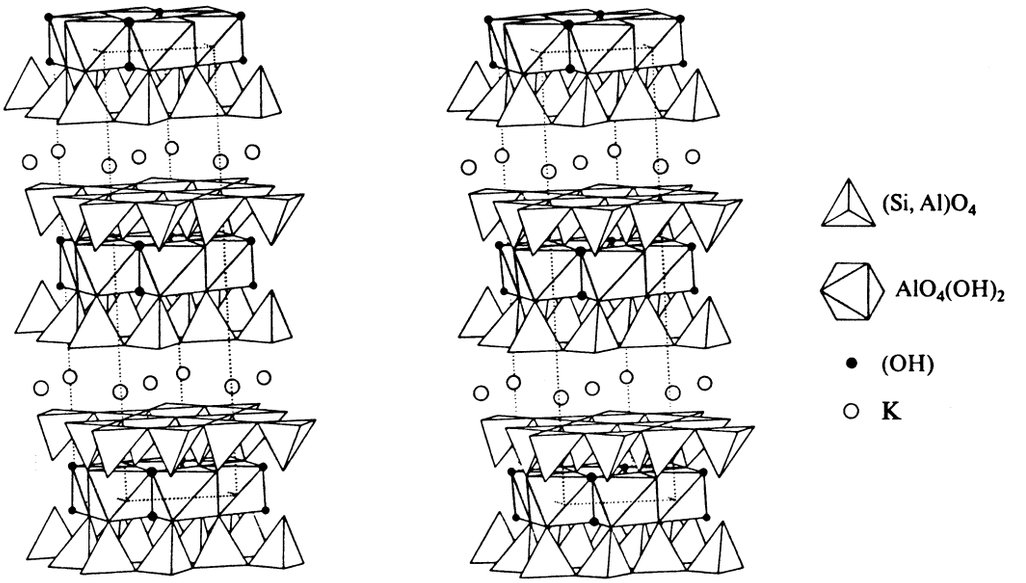

Fig. 9.2.2.12. Stereopair showing the sequence of sheets in the structures of the mica group (muscovite-2M_1, courtesy of Zoltai & Stout, 1985).

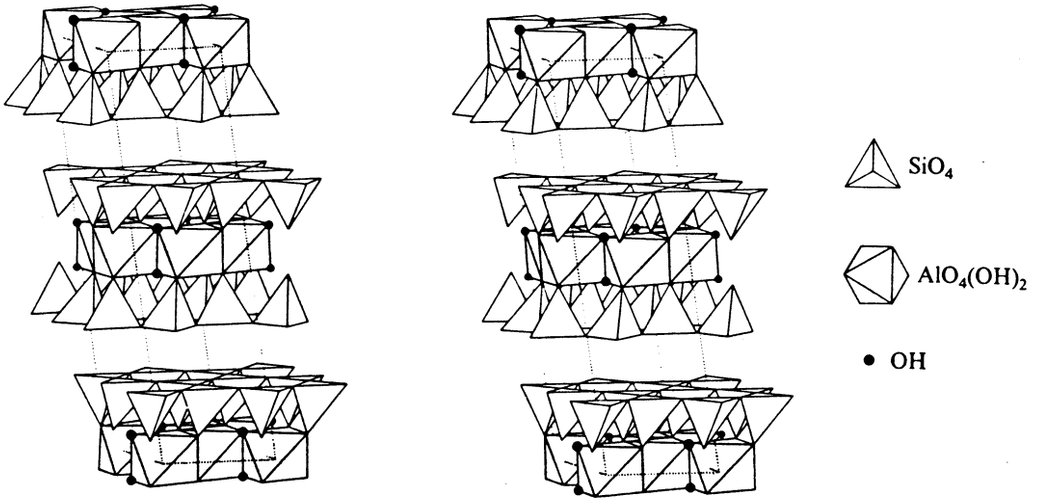

Fig. 9.2.2.13. Stereopair showing the sequence of sheets in the structures of the talc-pyrophyllite group (pyrophyllite-2M, courtesy of Zoltai & Stout, 1985).

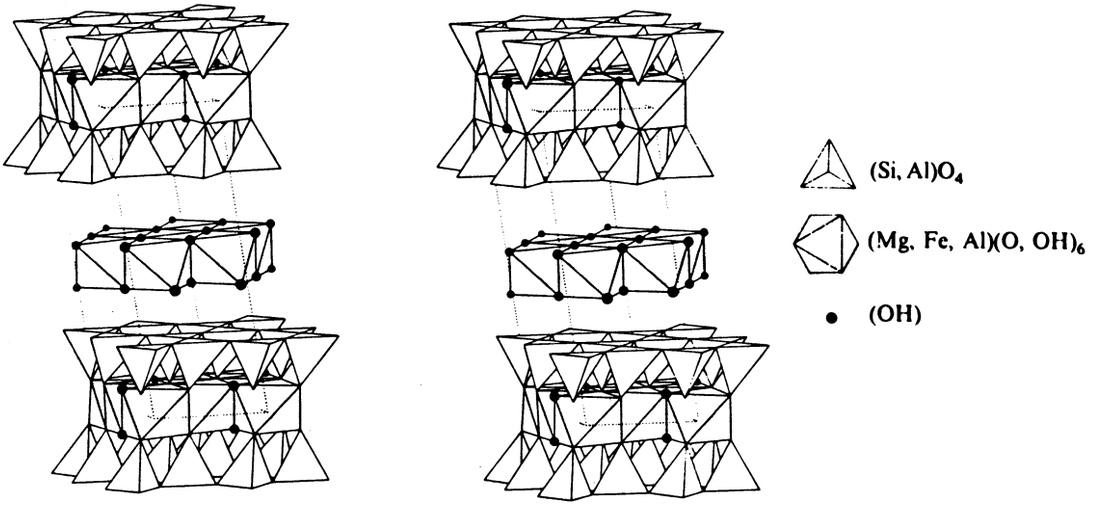

Fig. 9.2.2.14. Stereopair showing the sequence of sheets in the structures of the chlorite–vermiculite group (chlorite-1M, courtesy of Zoltai & Stout, 1985).

OD layer	layer group	subgroup of λ–τ oper.	N	F	Z
L_{2n+1}	$P(2/m)\,2/c\,2_1/m$	$P(2)cm$	4		1
			↘		↗
				2	
			↗		↘
L_{2n}	$P(1)\,2_1/c\,1$	$P(1)c1$	2		2.

Both polytypes are slightly desymmetrized. Since the shift between the origins of *Pyr* and *Tet* is irrational, stibivanite has no superposition structure and thus the diffraction patterns of its polytypes have no common set of family diffractions. Another remarkable point is that the recognition of these structures as OD structures of *layers* has nothing to do with their system of chemical bonds (see above).

9.2.2.3.3. γ-$Hg_3S_2Cl_2$

Among about 40 investigated crystals synthesized by Carlson (1967), not one was periodic. All diffraction patterns exhibited a common set of family diffractions, but the distribution of intensities along diffuse streaks varied from crystal to crystal (Ďurovič, 1968). The maxima on these streaks indicated in some cases a simultaneous presence of domains of three periodic polytypes – one system of diffuse maxima was always present and it was referred to a rectangular cell with $a = 9,328\,(5)$, $b = 16.28\,(1)$, $c = 9.081\,(6)$ Å with monoclinic symmetry. All crystals were more or less twinned, sometimes simulating orthorhombic symmetry in their diffraction patterns.

The superposition structure with $\mathbf{A} = \mathbf{a}$, $\mathbf{B} = \mathbf{b}/2$, $\mathbf{C} = 2\mathbf{c}$ and space group *Pbmm* was solved first. Here, a comparison of the family diffractions with the diffraction pattern of the α modification (Frueh & Gray, 1968) proved decisive. It turned out that only one kind of Hg atom contributed with half weight to the superposition structure. This means that only these atoms repeat in the actual structure with periods $\mathbf{b} = 2\mathbf{B}$ and $\mathbf{c} = 2\mathbf{C}$. All other atoms (in the first approximation) repeat with the periods of the superposition structure and thus do not contribute to the diffuse streaks.

The symmetry of the superposition structures is compatible with the OD groupoid family determined from systematic absences:

$A(2)$	m	m	
$\{(b_{1/2})$	$2_{1/2}$	$2\}$	
$\{(b_{1/2})$	$2_{1/2}$	$2\}$	category III,

where the subscripts 1/2 indicate translational components of $b/4$ (Dornberger-Schiff, 1964, pp. 41 ff.).

The solution of the structural principle thus necessitated only the correct location of the 'disordered' Hg atom in one of two

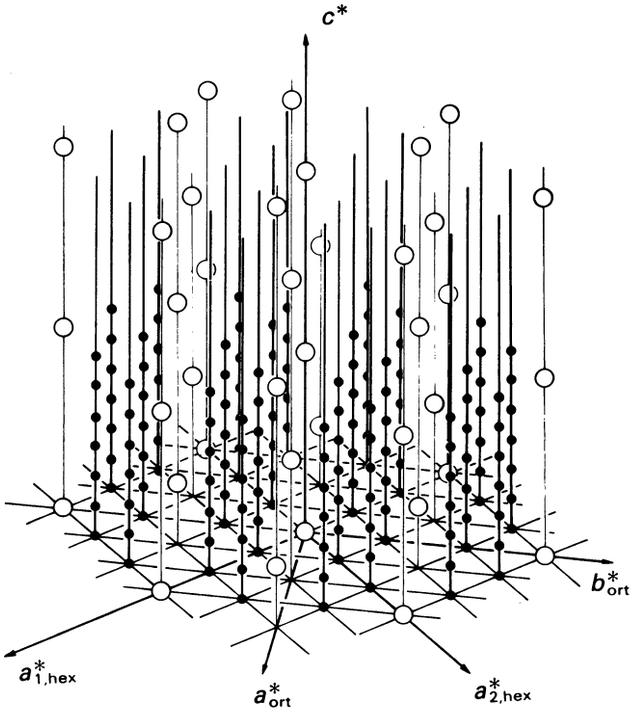

Fig. 9.2.2.15. Clinographic projection of the general scheme of a single-crystal diffraction pattern of hydrous phyllosilicates. Family diffractions are indicated by open circles and correspond in this case to a rhombohedral superposition structure. Only the part with $l \geq 0$ is shown.

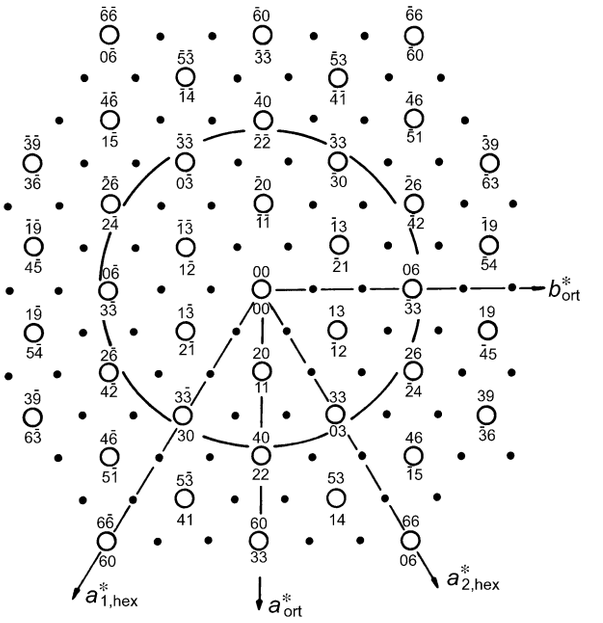

Fig. 9.2.2.16. Normal projection of the general scheme of a single-crystal diffraction pattern of hydrous phyllosilicates. Rows of family diffractions are indicated by open circles; the h, k indices refer to hexagonal (below) and orthogonal (above) axial systems.

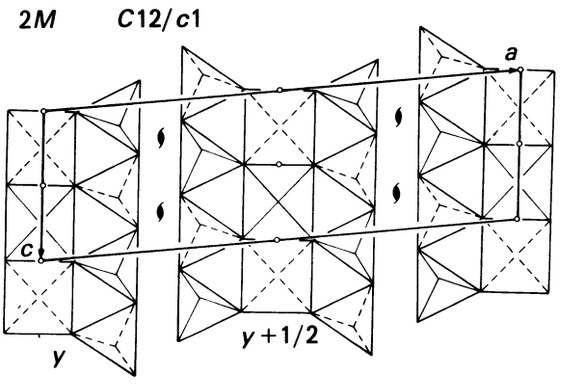

Fig. 9.2.2.17. The structure of stibivanite-2M. The unit cell is outlined and some relevant symmetry operations are indicated (after Merlino *et al.*, 1989).